Scientiae Radices, **4**(4), 287-306 (2025)

Full Paper

SciRad SCIENTIAE RADICES

Performing a Relative Interacting Atomic Energy Analysis of the Diels-Alder Reaction between Butadiene and Ethylene

Luis R. Domingo (1) ✉

(1) Independent research, Avd. Tirso de Molina 20, 46015, Valencia, Spain.

✉ Correspondence to: luisrdomingo@gmail.com

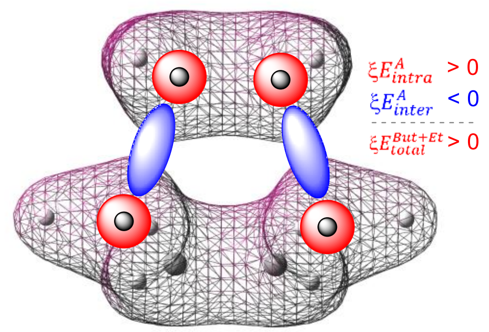

Main intra- and interatomic interactions at the non-polar **TSsyn**

Abstract: An energy decomposition analysis namely the Relative Interacting Atomic Energy (RIAE) was recently introduced within the Molecular Electron Density Theory. This energy decomposition analysis enables the study of the electronic intra- and interatomic interactions responsible for the activation energies of the organic reactions. Herein, a RIAE analysis of the unfavorable non-polar Diels-Alder reaction of butadiene with ethylene is carried out in order to determine the electronic factors responsible for its high activation energy. How the RIAE analysis is performed in the study of chemical organic reactions is explained.

Keywords: Relative Interacting Atomic Energy Analysis, Molecular Electron Density Theory, Chemical Organic Reactivity, Activation Energies, Diels-Alder reactions.

Received: 2025.09.29
Accepted: 2025.11.17
Published: 2025.12.19
DOI: 10.58332/scirad2025v4i4a03

Introduction

The two fundamental questions in organic chemistry are why and how the organic reactions take place. The development of quantum chemical tools such as Atom-in-Molecules [1,2] (AIM) and the Electron Localization Function [3] (ELF) at the end of the past century able to perform a topological analysis of the molecular electron density obtained by using the Kohn-Sham [4] (KS) formalism within the Density Functional Theory [5] (DFT) allowed to answer the question of how organic reactions take place. The implementation of the Bonding Evolution Theory [6] (BET) in 1997 allowed the establishment of the molecular mechanism of the more relevant organic reactions, but the question of why the reactions took place remained unresolved.

Several energy decomposition analyses based on the Morokuma-based energy decomposition scheme [7,8], such as the activation strain model [9] (ASM) and the distortion/interaction energy model [10,11] (DIEM) were proposed to resolve this relevant question.

After twenty years devoted to the theoretical study of organic chemical reactivity, Domingo proposed the Molecular Electron Density Theory [12] (MEDT) in 2016 to study chemical organic reactivity. This theory states that the energy cost associated with the reorganization of the molecular electron density along a reaction path determines the chemical reactivity. Consequently, the changes in electron density along the reaction paths, rather than molecular orbital (MO) interactions, as proposed by the Frontier Molecular Orbital (FMO) theory [13], should be investigated to better understand the chemical organic reactivity. Accordingly, MEDT rejects any outdated model based on the Morokuma-based energy decomposition schemes such as ASM [14,15] and DIEM [16,17] as they rely on MO components. MEDT has been extensively applied in recent years to investigate a wide range of organic reactions.

Very recently, an energy decomposition analysis based on the Interacting Quantum Atoms [18] (IQA), namely the Relative Interacting Atomic Energy [19] (RIAE), was introduced within MEDT. RIAE enables the analysis of electronic atomic interactions responsible for the activation energies of organic reactions, on which MEDT is founded [12]. The RIAE analysis has proved to be a powerful tool in the study of the intra-atomic and interatomic interactions responsible for the activation energies of organic reactions such as Diels-Alder (DA) reactions [20,21], [3+2] cycloaddition reactions [22], Alder-ene reactions [23] and more recently nucleophilic substitution reactions [24,25].

Herein, a RIAE analysis of the unfavorable DA reaction of butadiene **1** with ethylene **2** yielding cyclohexene **3** [26], which was proposed as the prototype of DA reactions, is performed (see Scheme 1) [27,28,29]. How the RIAE analysis is carried out in organic reactions is herein presented.

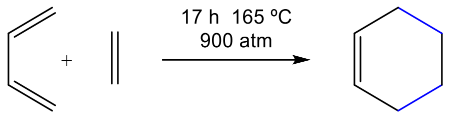

1 **2** **3**

Scheme 1. DA reaction between butadiene **1** with ethylene **2**.

Results and discussion

The present MEDT study has been divided in three sections: i) in section I the theoretical background of the RIAE analysis is presented; ii) in section II, how the RIAE analysis for the DA reaction between *s-cis* butadiene **1** with ethylene **2** is computationally performed, is discussed; and finally, iii) the RIAE analysis of the electronic factors responsible for the high activation energy associated with this DA reaction is completed.

I) Theoretical background of the RIAE Analysis

IQA [18], which is based on AIM [1,2], allows the partitioning of the total calculated KS energies [4] energies into the intra- and interatomic energy components. IQA divides the E_{total}^{IQA} total energies into two main energy contributions (see equation 1): the E_{intra}^{A} intra-atomic energies associated with the kinetic energies and electronic interactions of all particles inside each atom A, i.e. the nuclei and electrons (see equation 2), and the E_{inter}^{AB} interatomic energies associated with the interatomic electronic interactions of the particles of the atom A with the particles of atom B. The E_{inter}^{AB} interatomic energies are obtained by the sum of four electrostatic terms: the V_{ne}^{AB} and V_{en}^{AB} associated with nuclei-electron interactions, the V_{ee}^{AB} associated with the electron-electron interactions, and the V_{nn}^{AB} associated with nuclei-nuclei interactions (see equation 3). While the V_{ne}^{AB} and V_{en}^{AB} are negative and favorable, the V_{ee}^{AB} and V_{nn}^{AB} are positive and unfavorable.

$$E_{total}^{IQA} = \sum E_{intra}^{A} + \sum E_{inter}^{AB} \tag{1}$$

$$E_{intra}^{A} = T(A) + V_{ne}^{A} + V_{ee}^{A} \tag{2}$$

$$E_{inter}^{AB} = ½V_{ne}^{AB} + ½V_{en}^{AB} + ½V_{ee}^{AB} + V_{nn}^{AB} \tag{3}$$

Thanks to the additivity of the topological atoms [30], an interacting quantum fragment (IQF) approach was recently introduced [31]. This allows the IQA energies to be grouped into convenient frameworks in which the system is divided. This permits for a more meaningful chemical analysis of the interactions of the atoms belonging to the frameworks. In this sense, for the RIAE analysis [19], the atoms belonging to the transition state structure (TS) of the selected DA reaction are regrouped into two interacting frameworks f(X), related to the *s-cis* butadiene **1**, framework **A**, and the ethylene **2**, framework **B** [19].

By default, the sum of all IQA intra-atomic and interatomic energies belonging to the considered frameworks f(X) (where X represents either the **A** and **B** frameworks) at the TS, and those of the corresponding reagents at the ground states (GS), i.e. *s-cis* butadiene **1**, and ethylene **2**, is computed. The RIAEs, i.e., the relative ξE_{intra}^{X} intra-atomic, ξE_{inter}^{X} interatomic and ξE_{total}^{X} total energies, are obtained using equations 4-6. The symbol ξ denotes the IQA energy differences between those of the two-interacting frameworks at the TS, f(A) and f(B), and those at the GS of the reagents.

$$\xi E_{intra}^{X} = \Sigma E_{intra}^{f(X)[TS]} - \Sigma E_{intra}^{X[GS]} \tag{4}$$

$$\xi E_{inter}^{X} = \Sigma E_{inter}^{f(X)[TS]} - \Sigma E_{inter}^{X[GS]} \tag{5}$$

$$\xi E_{total}^{X} = \xi E_{intra}^{X} + \xi E_{inter}^{X} \tag{6}$$

This RIAE analysis provides a measure of how much the two interacting frameworks f(X) are destabilized (resulting in positive relative energies) or stabilized (resulting in negative relative energies) when going from the GS to the TS. The sum of the ξE_{total}^{X} energies of the two interacting frameworks, ξE_{total}^{A+B}, provides the RIAE activation energy of the DA reaction obtained through the present energy decomposition analysis [19,20].

II) Performing computationally the RIAE analysis of the DA reaction of *s-cis* butadiene 1 with ethylene 2

To perform the RIAE analysis, the potential energy surface of the DA reaction of *s-trans* butadiene **1** with ethylene **2** was firstly explored at the B3LYP/6-311G(d,p) level in gas phase. Butadiene **1** can be found in two conformations, the *s-trans* and the *s-cis*. The DA reaction between *s-cis* butadiene **1** and ethylene **2** takes place through a non-concerted one-step mechanism via the synchronous **TSsyn** (see Scheme 2) [32]. The B3LYP/6-311G(d,p) total and relative energies are given in Table 1 while the optimized geometry of **TSsyn** is shown in Figure 1.

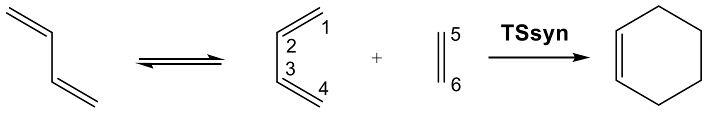

s-trans butadiene **1** *s-cis* butadiene **1** ethylene **2** **3**

Scheme 2. DA reaction between *s-cis* butadiene **1** with ethylene **2** via **TSsyn**.

The *s-trans* conformation of butadiene **1** is 3.51 kcal·mol^{-1} more stable than the *s-cis.* The activation energy associated to this DA reaction is 24.74 kcal·mol^{-1}, the reaction being strongly exothermic by 37.0 kcal·mol^{-1}. From the *s-cis* butadiene **1**, the activation energy associated with the formation of **TSsyn** is 21.2 kcal·mol^{-1}. The B3LYP/6-311G(d,p) computed activation energy is 2.8 kcal·mol^{-1} below the experimental value, 27.5 kcal·mol^{-1}.

Table 1. B3LYP/6-311G(d,p) total, E in a.u., and relative, ΔE in kcal·mol^{-1}, energies of the stationary points involved in the DA reaction of *s-trans* butadiene **1** with ethylene **2**.

	E	ΔE
s-trans butadiene **1**	-156.038505	
s-cis butadiene **1**	-156.032905	3.51
ethylene **2**	-78.613979	
TSsyn	-234.613061	24.74
3	-234.711500	-37.03

The optimized geometry of **TSsyn** shown in Figure 1 corresponds with a synchronous TS in which the electron density changes take place symmetrically. The distances between the two pairs of interacting Ci and Cj carbons are 2.249 Å. Considering that the formation of the C-C single bonds begins in the range 2.0 - 1.9 Å [33], these distances indicate that the formation of the new C-C single bond has not yet begun at **TSsyn**. On the other hand, the global electron density transfer [33] (GEDT) computed at this TSs, 0.00 e, characterizes the non-polar character of this DA reaction, being classified as a null electron density flux [34] (NEDF) reaction. This behavior accounts for the high activation energy associated with this non-polar DA reaction [35], which does not easily take place experimentally; see the reaction conditions in Scheme 1.

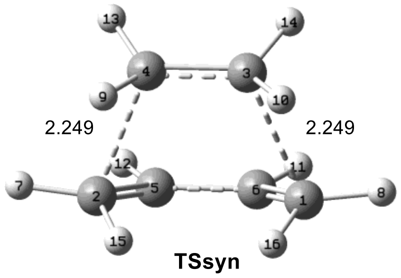

Fig. 1. B3LYP/6-311G(d,p) optimized geometry of **TSsyn** together with the atom numbering. The C-C distances between the two pairs of interacting atoms are given in Angstroms.

Finally, the AIM and ELF topological analyses of the electron density at **TSsyn** were performed. Figure 2 shows the 3D map of the electron density of this TS, the contour line maps of the Laplacian $\nabla^2\rho(r)$, and the ELF valence basins. AIM and ELF topological analysis of the electron density of **TSsyn** indicate that the formation of the new C-C single bonds has not yet begun at this TS. Thus, AIM shows the presence of two critical points (CPs) characterized by a low density, $r = 0.0509$, and a positive Laplacian, $\nabla^2\rho(r) = 0.0439$, while ELF indicates the absence of any new V(Ci,Cj) disynaptic basin between the interacting Ci and Cj carbons, associated with the new Ci-Cj single bonds created along this DA reaction.

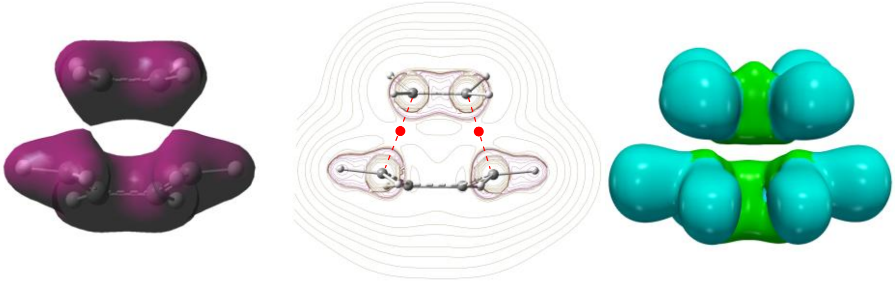
(a) (b) (c)

Fig. 2. Representations of (a) the map of the electron density of **TSsyn** with a surface isovalue of the electron density of 0.05; (b) the contour line maps of the Laplacian $\nabla^2\rho(r)$ of the electron density at **TSsyn**. The critical points CPs and the bond paths are marked in red; and (c) ELF valence basins.

Finally, the 3D map of the electron density of **TSsyn** shown in Figure 2 allows obtaining two appealing conclusions in agreement with the previous ELF and AIM analyses: i) the electron density of the frameworks **A** and **B** are not in contact at **TSsyn**; and ii) the electron density distribution at the four interacting carbons is not spherical. This behavior shows the structural changes of the four interacting carbons from a trigonal planar geometry at butadiene **1** and ethylene **2** at the GS to a tetrahedral one at cyclohexene **3**.

Once electronic structure of **TSsyn** was completely characterized, the IQA calculations for *s-cis* butadiene **1**, ethylene **2** and **TSsyn** were carried out. The information required to perform the RIAE analysis is found in the 'name.sum' files provided by AIMALL program [36]. These files contain all information about the IQA analysis. The main information required in the RIAE analysis are:

i) The intra-atomic interactions given in equation 2 which can be found in the section *Virial-Based Intraatomic and Interatomic Energy Contributions*. For ethylene **2** they are:

Virial-Based Intra-atomic and Interatomic Energy Contributions:

Atom A	E_Intra(A)	E_Inter(A)	Ee_Intra(A)	Ee_Inter(A)
C1	-3.7650172838E+01		-3.7650172838E+01	-2.3793643300E-01
C2	-3.7650197933E+01		-3.7650197933E+01	-2.3789070900E-01
H3	-4.6037679744E-01		-4.6037679744E-01	-1.5160129371E-01
H4	-4.6037596204E-01		-4.6037596204E-01	-1.5160155097E-01
H5	-4.6037539378E-01		-4.6037539378E-01	-1.5160197822E-01
H6	-4.6037642490E-01		-4.6037642490E-01	-1.5160149820E-01
Total	-7.7141875349E+01		-7.7141875349E+01	-1.0822334631E+00

ii) The interatomic interactions given in equation 3 which can be found in the section *IQA Atomic* c*ontributions to Interatomic ("Interaction") Energy*. For ethylene **2** they are:

Atom	IQA_Inter(A)	Vne(A,A')/2	Ven(A,A')/2	Vee(A,A')/2	Vnn(A)
C1	-4.8073974178E-01	-1.0980371756E+01	-1.1272058831E+01	1.0164871477E+01	1.1606819367E+01
C2	-4.8074692023E-01	-1.0980309843E+01	-1.1272154771E+01	1.0164898327E+01	1.1606819367E+01
H3	-1.2765219106E-01	-2.4742958775E+00	-2.3284134912E+00	2.1234038095E+00	2.5516533682E+00
H4	-1.2765215076E-01	-2.4742974355E+00	-2.3284031869E+00	2.1233951035E+00	2.5516533682E+00
H5	-1.2765244293E-01	-2.4742980488E+00	-2.3283990615E+00	2.1233912992E+00	2.5516533682E+00
H6	-1.2765227049E-01	-2.4742965014E+00	-2.3284093422E+00	2.1234002049E+00	2.5516533682E+00
Total	-1.4720957172E+00	-3.1857869462E+01	-3.1857838684E+01	2.8823360221E+01	3.3420252207E+01

iii) Finally, other relevant information is found in the section *IQA Diatomic "Interaction" Energy Components*, which provides an energy decomposition analysis of all the A-B interatomic interactions (see equation 3). This section can be very long; the data for **TSsyn** are given in Appendix 1.

Atom A	Atom B	E_IQA_Inter(A,B)	Vne(A,B)	Ven(A,B)	Vee(A,B)	Vnn(A,B)
C2	C1	-4.5745607198E-01	-1.3927261846E+01	-1.3927377982E+01	1.3044669223E+01	1.4352514533E+01
H3	C1	-5.6367152632E-03	-1.4936531229E+00	-1.4216035891E+00	1.4053246397E+00	1.5042953570E+00
H3	C2	-2.4642024482E-01	-2.8147813464E+00	-2.5950777598E+00	2.2371721182E+00	2.9262667432E+00
H4	C1	-2.4641298486E-01	-2.8147605776E+00	-2.5950672786E+00	2.2371481280E+00	2.9262667432E+00
H4	C2	-5.6365482638E-03	-1.4936693584E+00	-1.4215964465E+00	1.4053338997E+00	1.5042953570E+00
H4	H3	-2.4018948938E-04	-2.0675854762E-01	-2.0675748084E-01	1.9897870019E-01	2.1429713878E-01
H5	C1	-5.6376289092E-03	-1.4936628247E+00	-1.4215925257E+00	1.4053223645E+00	1.5042953570E+00
H5	C2	-2.4642611428E-01	-2.8147988186E+00	-2.5950640832E+00	2.2371700444E+00	2.9262667432E+00
H5	H3	-2.3440009352E-03	-2.6939618986E-01	-2.6939490466E-01	2.4966406258E-01	2.8678303102E-01
H5	H4	-6.4979882744E-04	-1.6399012597E-01	-1.6398978096E-01	1.5566564164E-01	1.7166446646E-01
H6	C1	-2.4642483020E-01	-2.8147792830E+00	-2.5950745118E+00	2.2371622214E+00	2.9262667432E+00
H6	C2	-5.6396593468E-03	-1.4936820305E+00	-1.4215996601E+00	1.4053466743E+00	1.5042953570E+00
H6	H3	-6.4987033610E-04	-1.6399088529E-01	-1.6399054215E-01	1.5566709065E-01	1.7166446646E-01
H6	H4	-2.3438461232E-03	-2.6939503136E-01	-2.6939607854E-01	2.4966423276E-01	2.8678303102E-01
H6	H5	-2.4026749502E-04	-2.0675681796E-01	-2.0675788060E-01	1.9897729231E-01	2.1429713878E-01

The intra- and interatomic interactions of the atoms belonging to ethylene **2** demanded for the RIAE analysis are summarized in Table 2.

Table 2. Intra- and interatomic interactions, in a.u., of the atoms belonging to ethylene **2**.

Atom A	E_IQA_Intra(A)
C1	-3.7650172839E+01
C2	-3.7650197932E+01
H3	-4.6037679744E-01
H4	-4.6037596208E-01
H5	-4.6037539376E-01
H6	-4.6037642486E-01
Total	-7.7141875349E+01
Atom A	E_IQA_Inter(A)
C1	-4.8073974178E-01
C2	-4.8074692023E-01
H3	-1.2765219106E-01
H4	-1.2765215076E-01
H5	-1.2765244293E-01
H6	-1.2765227049E-01
Total	-1.4720957172E+00

The analysis shown for ethylene **2** should be also performed for *s-cis* butadiene **1** and **TSsyn**. IQA gives all these energies in a.u. The intra- and interatomic interactions of the three species as shown in Table 2 are transferred to an Excel sheet as shows Figure 3:

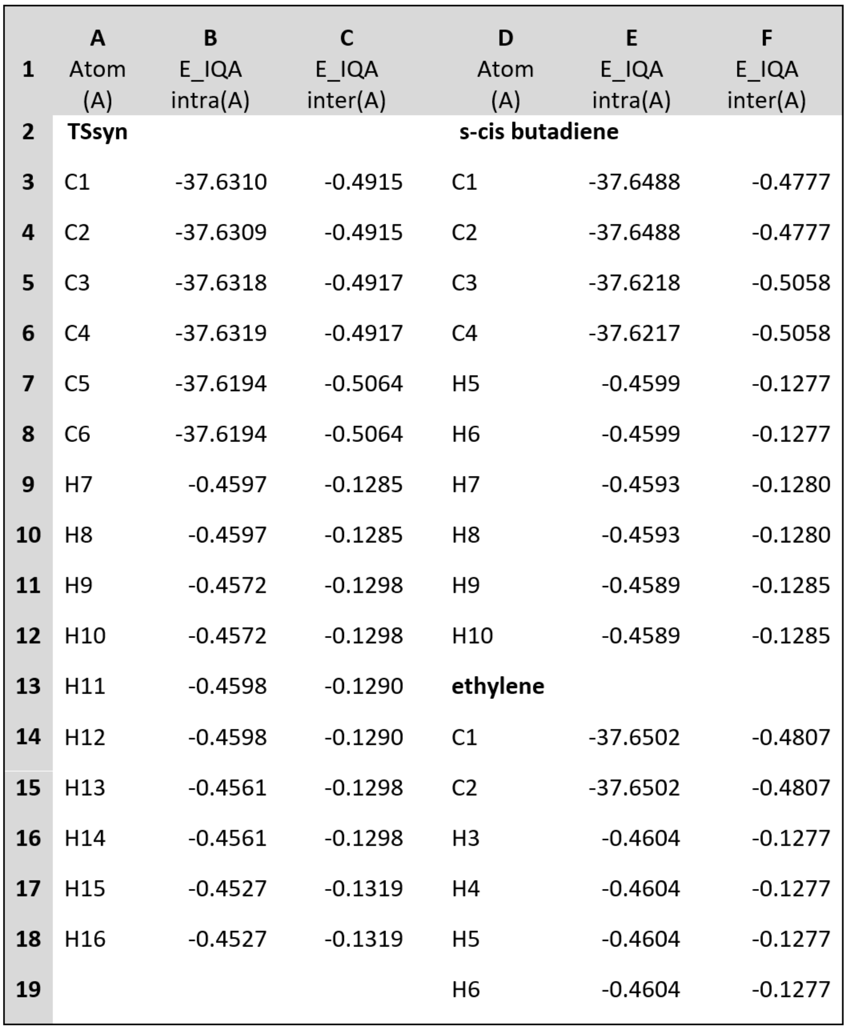

	A	B	C	D	E	F
1	Atom (A)	E_IQA intra(A)	E_IQA inter(A)	Atom (A)	E_IQA intra(A)	E_IQA inter(A)
2	**TSsyn**			**s-cis butadiene**		
3	C1	-37.6310	-0.4915	C1	-37.6488	-0.4777
4	C2	-37.6309	-0.4915	C2	-37.6488	-0.4777
5	C3	-37.6318	-0.4917	C3	-37.6218	-0.5058
6	C4	-37.6319	-0.4917	C4	-37.6217	-0.5058
7	C5	-37.6194	-0.5064	H5	-0.4599	-0.1277
8	C6	-37.6194	-0.5064	H6	-0.4599	-0.1277
9	H7	-0.4597	-0.1285	H7	-0.4593	-0.1280
10	H8	-0.4597	-0.1285	H8	-0.4593	-0.1280
11	H9	-0.4572	-0.1298	H9	-0.4589	-0.1285
12	H10	-0.4572	-0.1298	H10	-0.4589	-0.1285
13	H11	-0.4598	-0.1290	**ethylene**		
14	H12	-0.4598	-0.1290	C1	-37.6502	-0.4807
15	H13	-0.4561	-0.1298	C2	-37.6502	-0.4807
16	H14	-0.4561	-0.1298	H3	-0.4604	-0.1277
17	H15	-0.4527	-0.1319	H4	-0.4604	-0.1277
18	H16	-0.4527	-0.1319	H5	-0.4604	-0.1277
19				H6	-0.4604	-0.1277

Fig. 3. IQA intra- and interatomic energies, in a.u., of **TSsyn**, *s-cis* butadiene **1** and ethylene **2**.

Then, the intra- and interatomic energies of **TSsyn** are regrouped into the frameworks f(**A**) and f(**B**), and the atoms are positioned in the same row that the corresponding atoms belonging to *s-cis* butadiene **1** and ethylene **2** as shows Figure 4. Note that the atom numbering at **TSsyn** and the two reagents is based on a graphical representation of the input files used for the IQA calculations (see Figure 1 for **TSsyn**).

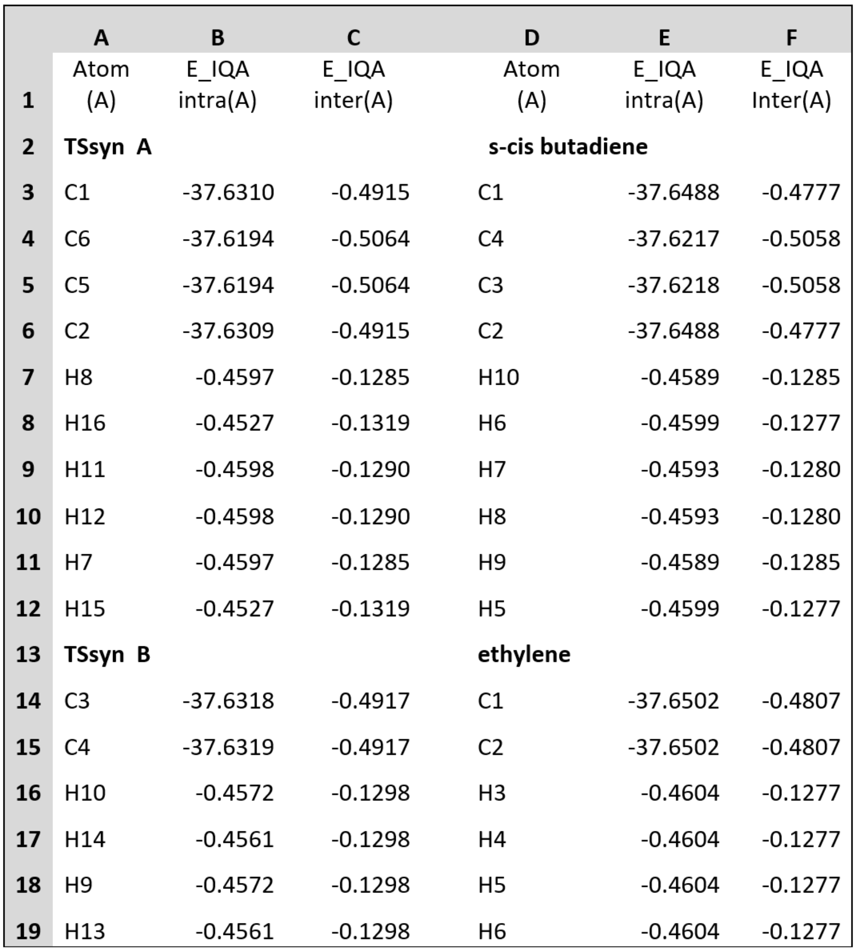

	A	B	C	D	E	F
1	Atom (A)	E_IQA intra(A)	E_IQA inter(A)	Atom (A)	E_IQA intra(A)	E_IQA Inter(A)
2	**TSsyn A**			**s-cis butadiene**		
3	C1	-37.6310	-0.4915	C1	-37.6488	-0.4777
4	C6	-37.6194	-0.5064	C4	-37.6217	-0.5058
5	C5	-37.6194	-0.5064	C3	-37.6218	-0.5058
6	C2	-37.6309	-0.4915	C2	-37.6488	-0.4777
7	H8	-0.4597	-0.1285	H10	-0.4589	-0.1285
8	H16	-0.4527	-0.1319	H6	-0.4599	-0.1277
9	H11	-0.4598	-0.1290	H7	-0.4593	-0.1280
10	H12	-0.4598	-0.1290	H8	-0.4593	-0.1280
11	H7	-0.4597	-0.1285	H9	-0.4589	-0.1285
12	H15	-0.4527	-0.1319	H5	-0.4599	-0.1277
13	**TSsyn B**			**ethylene**		
14	C3	-37.6318	-0.4917	C1	-37.6502	-0.4807
15	C4	-37.6319	-0.4917	C2	-37.6502	-0.4807
16	H10	-0.4572	-0.1298	H3	-0.4604	-0.1277
17	H14	-0.4561	-0.1298	H4	-0.4604	-0.1277
18	H9	-0.4572	-0.1298	H5	-0.4604	-0.1277
19	H13	-0.4561	-0.1298	H6	-0.4604	-0.1277

Fig.4. Reorganization of the IQA intra- and interatomic energies of **TSsyn** into the two frameworks in which the TS has been divided.

Finally, the relative ξE^{X}_{intra} intra-atomic and ξE^{X}_{inter}interatomic energies, in red, and the ξE^{X}_{total} total atomic energies, in blue, are computed using equations 4, 5 and 6, respectively, where X are the framework f(**A**) or *s-cis* butadiene **1**, and framework f(**B**) or ethylene **2** as shows Figure 5.

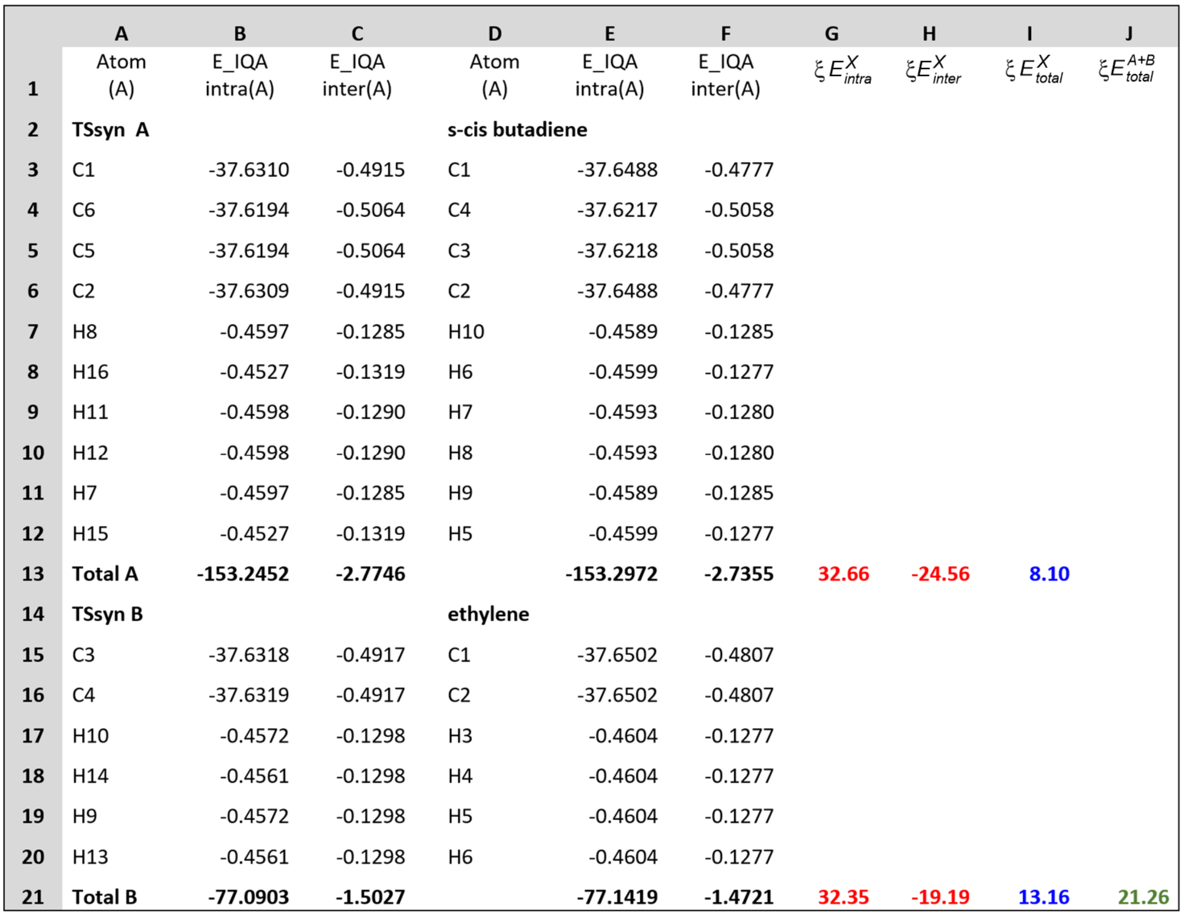

	A	B	C	D	E	F	G	H	I	J
1	Atom (A)	E_IQA intra(A)	E_IQA inter(A)	Atom (A)	E_IQA intra(A)	E_IQA inter(A)	ξE^{X}_{intra}	ξE^{X}_{inter}	ξE^{X}_{total}	ξE^{A+B}_{total}
2	**TSsyn A**			**s-cis butadiene**						
3	C1	-37.6310	-0.4915	C1	-37.6488	-0.4777				
4	C6	-37.6194	-0.5064	C4	-37.6217	-0.5058				
5	C5	-37.6194	-0.5064	C3	-37.6218	-0.5058				
6	C2	-37.6309	-0.4915	C2	-37.6488	-0.4777				
7	H8	-0.4597	-0.1285	H10	-0.4589	-0.1285				
8	H16	-0.4527	-0.1319	H6	-0.4599	-0.1277				
9	H11	-0.4598	-0.1290	H7	-0.4593	-0.1280				
10	H12	-0.4598	-0.1290	H8	-0.4593	-0.1280				
11	H7	-0.4597	-0.1285	H9	-0.4589	-0.1285				
12	H15	-0.4527	-0.1319	H5	-0.4599	-0.1277				
13	**Total A**	**-153.2452**	**-2.7746**		**-153.2972**	**-2.7355**	**32.66**	**-24.56**	**8.10**	
14	**TSsyn B**			**ethylene**						
15	C3	-37.6318	-0.4917	C1	-37.6502	-0.4807				
16	C4	-37.6319	-0.4917	C2	-37.6502	-0.4807				
17	H10	-0.4572	-0.1298	H3	-0.4604	-0.1277				
18	H14	-0.4561	-0.1298	H4	-0.4604	-0.1277				
19	H9	-0.4572	-0.1298	H5	-0.4604	-0.1277				
20	H13	-0.4561	-0.1298	H6	-0.4604	-0.1277				
21	**Total B**	**-77.0903**	**-1.5027**		**-77.1419**	**-1.4721**	**32.35**	**-19.19**	**13.16**	**21.26**

Fig.5. Computation of the relative ξE^{X}_{intra} intra-atomic, ξE^{X}_{inter} interatomic, and ξE^{X}_{total} total atomic energies, in kcal·mol^{-1}, of the frameworks f(**A**) and f(**B**).

The sum of the ξE^{X}_{total} total atomic energies of the two frameworks, in blue, provides the computed ξE^{A+B}_{total} RIAE activation energy, in green, 21.26 kcal·mol^{-1}. As can be seen, a deviation of 0.04 kcal·mol^{-1} between the computed KS activation energies given in Table 1 and the ξE^{A+B}_{total} RIAE activation energies is obtained (see Table 3).

Table 3. B3LYP/6-311G(d,p) total, E in a.u., and relative, ΔE in kcal·mol^{-1}, DFT KS and IQA energies of *s-cis* butadiene **1**, ethylene **2**, and **TSsyn**.

	DFT KS calculations		IQA calculations		
	E	ΔE	E	ΔE	deviation
s-cis butadiene **1**	-156.032905		-156.032732		
ethylene **2**	-78.613979		-78.613971		
TSsyn	-234.613061	21.22	-234.612825	21.26	0.04

Finally, the data obtained for the RIAE analysis are presented as exposed in Table 4. Figure 6 shows a schematic representation of the RIAE energies.

Table 4. Gas-phase intra-atomic energies, ξE_{intra}^{X}, interatomic energies, ξE_{inter}^{X}, and total energies, ξE_{total}^{X}, in kcal·mol^{-1}, calculated using B3LYP/6-311G(d,p) level for the butadiene and ethylene frameworks, at **TSsyn** relative to their GSs. The sum of the ξE_{total}^{X} total energies of both frameworks, denoted as ξE_{total}^{But+Et}, represents the RIAE activation energy. Energies are given in kcal·mol^{-1}.

	$f(\mathrm{X})$	ξE_{intra}^{X}	ξE_{inter}^{X}	ξE_{total}^{X}	ξE_{total}^{But+Et}
TSsyn	But	32.66	-24.56	8.10	21.26
	Et	33.35	-18.16	13.16	

As shown Figure 6, the unfavorable ξE_{total}^{But} and ξE_{total}^{Et} total energies associated with the butadiene **A** and ethylene **B** frameworks are responsible for the high RIAE activation energy associated with this unfavorable non-polar DA reaction [35]. As can be seen, the unfavorable ξE_{total}^{Et} total energies associated with the ethylene framework **B** contributes with a higher extent to the RIAE activation energy. This graph is a pertinent tool when several organic reactions are compared. See references 19-25.

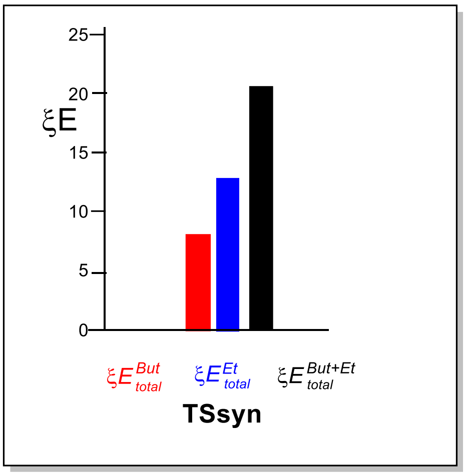

Fig.6. Graphical representation of the total energies, ξE_{total}^{But}, ξE_{total}^{Et}, and ξE_{total}^{But+Et} for **TSsyn** given in Table 4. ξE_{total}^{But+Et} value corresponds to the RIAE activation energy of this non-polar DA reaction. ξE_{total}^{X} energies for the But and Et frameworks are shown in red and blue, respectively, while the black bar represents the ξE_{total}^{But+ET} relative energies. Energies are reported in kcal·mol^{-1}.

*III) RIAE analysis of the electronic factors responsible for the high activation energy associated with the non-polar DA reaction between s-cis butadiene **1** and ethylene **2**.*

Finally, a RIAE analysis of the electronic factors responsible for the high activation energy associated with the non-polar DA reaction between *s-cis* butadiene **1** and ethylene **2** is conducted.

First, from the data given in Table 4, the following appealing conclusions can be obtained: i) on going from the GS to **TSsyn**, the two frameworks **A** and **B** are destabilized by

8.10 and 13.16 kcal·mol^{-1}, the smaller ethylene framework **B** being more destabilized (see Figure 6); ii) the ξE^{X}_{intra} intra-atomic energies are strongly destabilizing, while the ξE^{X}_{inter} interatomic energies are stabilizing in both frameworks; and finally, iii) the high RIAE activation energy associated with this DA reaction, ξE^{But+Et}_{total} = 21.26 kcal·mol^{-1}, accounts for the drastic experimental conditions required for this non-polar DA reaction (see Scheme 1).

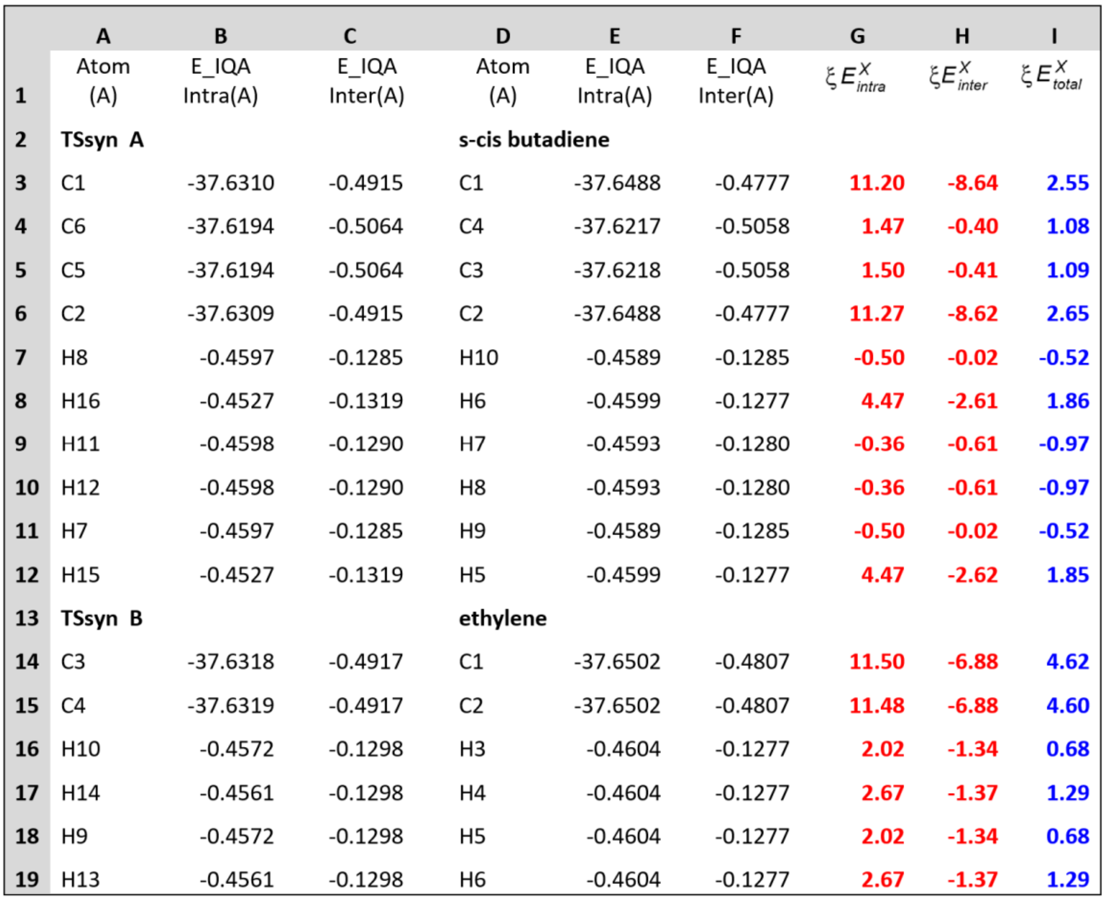

	A	B	C	D	E	F	G	H	I
1	Atom (A)	E_IQA Intra(A)	E_IQA Inter(A)	Atom (A)	E_IQA Intra(A)	E_IQA Inter(A)	ξE^{X}_{intra}	ξE^{X}_{inter}	ξE^{X}_{total}
2	**TSsyn A**			**s-cis butadiene**					
3	C1	-37.6310	-0.4915	C1	-37.6488	-0.4777	11.20	-8.64	2.55
4	C6	-37.6194	-0.5064	C4	-37.6217	-0.5058	1.47	-0.40	1.08
5	C5	-37.6194	-0.5064	C3	-37.6218	-0.5058	1.50	-0.41	1.09
6	C2	-37.6309	-0.4915	C2	-37.6488	-0.4777	11.27	-8.62	2.65
7	H8	-0.4597	-0.1285	H10	-0.4589	-0.1285	-0.50	-0.02	-0.52
8	H16	-0.4527	-0.1319	H6	-0.4599	-0.1277	4.47	-2.61	1.86
9	H11	-0.4598	-0.1290	H7	-0.4593	-0.1280	-0.36	-0.61	-0.97
10	H12	-0.4598	-0.1290	H8	-0.4593	-0.1280	-0.36	-0.61	-0.97
11	H7	-0.4597	-0.1285	H9	-0.4589	-0.1285	-0.50	-0.02	-0.52
12	H15	-0.4527	-0.1319	H5	-0.4599	-0.1277	4.47	-2.62	1.85
13	**TSsyn B**			**ethylene**					
14	C3	-37.6318	-0.4917	C1	-37.6502	-0.4807	11.50	-6.88	4.62
15	C4	-37.6319	-0.4917	C2	-37.6502	-0.4807	11.48	-6.88	4.60
16	H10	-0.4572	-0.1298	H3	-0.4604	-0.1277	2.02	-1.34	0.68
17	H14	-0.4561	-0.1298	H4	-0.4604	-0.1277	2.67	-1.37	1.29
18	H9	-0.4572	-0.1298	H5	-0.4604	-0.1277	2.02	-1.34	0.68
19	H13	-0.4561	-0.1298	H6	-0.4604	-0.1277	2.67	-1.37	1.29

Fig.7. Computation of the relative ξE^{X}_{intra} intra-atomic, ξE^{X}_{inter}interatomic, and ξE^{X}_{total} total atomic energies, in kcal·mol^{-1}, of the frameworks f(**A**) and f(**B**).

A further detailed analysis of the ξE^{A}_{intra} intra-atomic and ξE^{A}_{inter} interatomic energies for each atom A of the two frameworks **A** and **B**, computed by using equations 7 and 8 and showed in Figure 7, indicates that although the ξE^{A}_{inter} interatomic energies of the four interacting carbons of the butadiene and ethylene frameworks are stabilizing by -8.6 and -6.8 kcal·mol^{-1}, respectively, the ξE^{A}_{intra} intra-atomic energies are more destabilizing by 11.2 and 11.5 kcal·mol^{-1}. Interestingly, the two central carbons of the butadiene framework (**A**), which remain trigonal planar along the DA reaction, are only intra-atomically destabilized by 1.5 kcal·mol^{-1} (see Figure 7).

$$\xi E_{intra}^{A} = E_{intra}^{A\,[TS[} - E_{intra}^{A\,[GS]} \tag{7}$$

$$\xi E_{inter}^{A} = E_{inter}^{A\,[TS]} - E_{inter}^{A\,[GS]} \tag{8}$$

Figure 8, which shows graphically the more relevant ξE_{intra}^{X} intra-atomic, in red, and ξE_{inter}^{X} interatomic, in blue, interactions at **TSsyn**, reveals two interesting observations: i) the more unfavorable ξE_{intra}^{A} intra-atomic interactions are found at the four interacting carbons, which are shifting from a trigonal planar arrangement to a tetrahedral one. Note that the two central carbons of the butadiene framework (**A**), which remain trigonal planar along the DA reaction, are slightly destabilized; and ii) the more favorable ξE_{inter}^{A} interatomic interactions are found in the non-bonding regions involving the two pairs of interacting Ci and Cj carbons. As the 3D map of the electron density of the non-polar **TSsyn** shows, the electron density of each one the two pairs of interacting Ci and Cj carbons is polarized towards the other carbon (see the green pointed circles in Figure 4). This behavior is a consequence of the more favorable V_{eN}^{AB} and V_{en}^{BA} interatomic interactions that the unfavorable V_{ee}^{AB} ones.

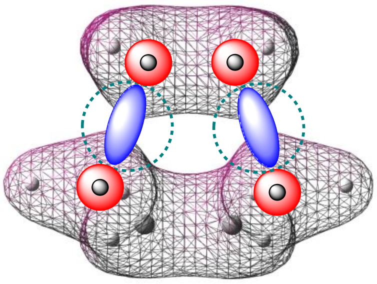

TSsyn

Fig.8. Representation of the 3D map of the electron density of the non-polar **TSsyn**, showing the main unfavorable ξE_{intra}^{A} intra-atomic, in red, and favorable ξE_{inter}^{A} interatomic, in blue, interactions contributing to the RIAE activation energy. The green pointed circles show the atomic electron density polarization.

The IQA diatomic A-B interaction energy components given in Appendix I permit to understand the origin of the favorable ξE_{inter}^{AB} interatomic energies between the two pairs of interacting Ci and Cj carbons at **TSsyn**. The corresponding E_{inter}^{AB} interatomic energies between the interacting C1-C3 and C2-C4 carbons are given in Table 4. As can be seen, in spite of the very high positive repulsive Vee(A,B) and Vnn(A,B) interactions between these interacting carbons, the negative attractive Vne(A,B) and Ven(A,B) interactions are higher, and consequently, the total E_{inter}^{AB} interatomic interactions between the two pairs of interacting Ci and Cj carbons are favorable by -47.02 kcal·mol^{-1}.

Table 5. IQA diatomic A-B interaction energy components, in kcal·mol^{-1}, between the interacting C1-C3 and C2-C4 carbons.

Atom A	Atom B	E_{inter}^{AB}	Vne(A,B)	Ven(A,B)	Vee(A,B)	Vnn(A,B)
C3	C1	-47.02	-5377.40	-5367.20	5382.72	5314.85
C4	C2	-47.02	-5377.40	-5367.20	5382.72	5314.85

Finally, both BET and RIAE studies of organic reactions involving the formation of a C-C single bond have shown that although the ξE_{total}^{A+B} RIAE activation energies are positive and consequently unfavorable, E_{inter}^{AB} inter-atomic energies involving the two interacting carbons are negative and favorable [19-23]. These net favorable C-C interactions, which occur before the formation of new C-C single bonds, refute the concept of 'Pauli repulsions', which was developed within the ASM [9], proposing that they control organic reactions [37]. Note that although the hypothetical 'Pauli repulsions' decrease with the increase of C-C distances, the favorable E_{inter}^{AB} interatomic energies decrease more significantly.

Conclusions

A RIAE analysis of the electronic factors responsible for high activation energy associated with the non-polar DA reaction between butadiene **1** and ethylene **2** has been carried out within MEDT at the B3LYP/6-311G(d,p) computational level. This reaction takes place through a non-concerted one-step mechanism via a synchronous **TSsyn**. The GEDT computed at this TS, 0.00 e, shows the non-polar character of this DA reaction, classified as NEDF, thus justifying the high activation energy of the reaction.

AIM and ELF topological analyses of the electron density distribution at **TSsyn** indicate that the formation of the new Ci-Cj single bond has not yet begun. On the other hand, both the 3D map of the electron density and the analysis of the contour line maps of the Laplacian $\nabla^2\rho$(r) show that the spheric electron density distribution of the interacting carbons at the GS of the reagents is polarized as a consequence of the continuous modification of the electron density distribution of these carbons, which change from a trigonal planar geometry at the GS to a tetrahedral one at the final cyclohexene **3**.

The present RIAE analysis of **TSsyn** permits to obtain some appealing conclusions: i) the changes in electron density at both butadiene and ethylene frameworks are energetically unfavorable, contributing to the high ξE_{total}^{But+Et} RIAE activation energy of this non-polar DA reaction; ii) the changes in electron density at the smaller ethylene framework are more unfavorable than those at the butadiene framework; iii) analysis of the total ξE_{intra}^{X} intra-atomic and the ξE_{inter}^{X} interatomic energies indicate that on going from GS to TS, while the former are destabilizing, the latter are stabilizing; iv) analysis of the factors contributing to the unfavorable ξE_{intra}^{X} intra-atomic energies shows that the E_{intra}^{Ci} energies associated with the two pairs of interacting carbons are the main electronic factors responsible for the high activation energy of this DA reaction; and finally, v) analysis of the factor contributing to the favorable ξE_{inter}^{AB} interatomic energies shows that the E_{inter}^{CiCj} interatomic energies associated with the two pairs of Ci and Cj interacting carbons are the main electronic factors which contribute to diminish the unfavorable ξE_{intra}^{X} intra-atomic energies. The present RIAE analysis of the unfavorable DA reaction under study allows us to know the electronic factors responsible for the high activation energy of this non-polar DA reaction. The RIAE analyses helps us to understand why organic reactions energetically occur.

Finally, the favorable E_{inter}^{CiCj} interatomic energies involving the two pairs of Ci and Cj interacting carbons make it possible to refute the concept of 'Pauli repulsions', developed within the ASM [7]; although the unfavorable hypothetical 'Pauli repulsions' decrease with the increase of the Ci-Cj distances, the more favorable E_{inter}^{CiCj} interatomic energies decrease more significantly.

Computational Methods

The B3LYP functional [38,39], together with the standard 6-311G(d,p) basis set [40], which includes d-type polarization for second-row elements and p-type polarization functions for hydrogens, was used throughout this MEDT study. Details of the search and characterization of the stationary points involved in these DA reactions are given in references 14-18. The GEDT [33] values were computed using the equation GEDT(f(X)) = $\Sigma q_{f(X)}$, where q are the natural charges [41,42] of the atoms belonging to one of the two frameworks f(X) at the TS geometries. The Gaussian 16 suite of programs was used to perform the calculations [43]. Molecular geometries were visualized by using the GaussView program [44]. ELF analyses of the B3LYP/6-311G(d,p) monodeterminantal wavefunctions were performed with the TopMod package [45] employing a cubic grid with a step size of 0.1. The IQA analysis was performed with the AIMAll package [36] using the corresponding B3LYP/6-311G(d,p) monodeterminantal pseudo-wavefunctions. Note that the AIMAll package only allows the use of the B3LYP [38,39] and the M06-2X [46] functionals.

References

[1] Bader, R.F.W.; Tang, Y.H.; Tal, Y.; Biegler-König, F.W. Properties of atoms and bonds in hydrocarbon molecules. *J. Am. Chem. Soc.*, **1982**, *104*, 946–952.

[2] Bader, R.F.W. In *Atoms in Molecules: A Quantum Theory*. Oxford University Press, Oxford, New York, 1994.

[3] Becke, A.D.; Edgecombe, K.E. A simple measure of electron localization in atomic and molecular-systems. *J. Chem. Phys.*, **1990**, *92*, 5397–5403.

[4] Kohn, W.; Sham, L. J. Self-consistent equations including exchange and correlation effects. *Phys. Rev. B*, **1965**, *140*, A1133-A1138.

[5] Hohenberg, P.; Kohn, W. Inhomogeneous Electron Gas. *Physical Review*, **1964**, *136*, B864–B871.

[6] Krokidis, X.; Noury, S.; Silvi, B. Characterization of Elementary Chemical Processes by Catastrophe Theory. *J. Phys. Chem. A*, **1997**, *101*, 7277–7282.

[7] Kitaura, K.; Morokuma, K. A new energy decomposition scheme for molecular interactions within the Hartree-Fock approximation. *Int. J. Quantum Chem.*, **1976**, *10*, 325-340.

[8] Morokuma, K.; Kitaura, K. In *Chemical Applications of Atomic and Molecular Electrostatic Potentials*. New York, Plenum., 1981, pp. 215–242.

[9] Bickelhaupt, F.M. Understanding reactivity with Kohn–Sham molecular orbital theory: E2–SN2 mechanistic spectrum and other concepts. *J. Comput. Chem.*, **1999**, *20*, 114–128.

[10] Ess, D. H.; K. N. Houk, K. N. Distortion/Interaction Energy Control of 1,3-Dipolar Cycloaddition Reactivity. *J. Am. Chem. Soc.*, **2007**, *129*, 10646-10647.

[11] Ess, D. H.; Houk, K. N. Theory of 1,3-Dipolar Cycloadditions: Distortion/ Interaction and Frontier Molecular Orbital Models. *J. Am. Chem. Soc.*, **2008**, *130*, 10187-10198.

[12] Domingo, L.R. Molecular Electron Density Theory: A Modern View of Reactivity in Organic Chemistry. *Molecules*, **2016**, *21*, 1319.

[13] Fukui, K. In *Molecular Orbitals in Chemistry, Physics, and Biology*, New York, 1964.

[14] Domingo, L.R.; Pérez, P. The Lithium Cation Catalysed Benzene Diels-Alder reaction. Insights on the Molecular Mechanism within the Molecular Electron Density Theory. *J. Org. Chem.*, **2020**, *85*, 13121–13132.

[15] Domingo, L.R.; Pérez, P.; Ríos-Gutiérrez, M.; José Aurell, M. A Molecular Electron Density Theory Study of Hydrogen Bond Catalysed Polar Diels–Alder Reactions of α,β-unsaturated Carbonyl Compounds. *Tetrahedron Chem.*, **2024**, *10*, 100064.

[16] Domingo, L.R.; Ríos-Gutiérrez, M.; Pérez, P. A Molecular Electron Density Theory Study of the [3+2] Cycloaddition Reaction of Nitrones with Strained Allenes. *RSC Adv.*, **2017**, *7*, 26879 – 26887.

[17] Domingo, L.R.; Ríos-Gutiérrez, M.; Pérez, P. Unveiling the Role of the Strain of Cyclohexyne in [3+2] Cycloaddition Reactions through the Molecular Electron Density Theory. *Org. Biomol. Chem.*, **2019**, 17, 498-508.

[18] Blanco, M. A.; Martín Pendás, A.; Francisco, E. Interacting Quantum Atoms: A Correlated Energy Decomposition Scheme Based on the Quantum Theory of Atoms in Molecules. *J. Chem. Theory Comput.*, **2005**, *1*, 1096–1109.

[19] Domingo, L. R.; Ríos-Gutiérrez, M.; Pérez, P. Understanding the Electronic Effects of Lewis Acid Catalysts in Accelerating Polar Diels–Alder Reactions. *J. Org. Chem.*, **2024**, *89*, 12349−12359.

[20] Domingo, L. R.; Ríos-Gutiérrez, M. Revealing the Decisive Role of Global Electron Density Transfer in the Reaction Rate of Polar Organic Reactions within Molecular Electron Density Theory. *Molecules*, **2024**, *29*, 1.

[21] Domingo, L.R.; Pérez, P. Intramolecular versus Intermolecular Diels-Alder Reactions: Insights from Molecular Electron Density Theory. *Molecules*, **2025**, *30*, 2052.

[22] Domingo, L. R.; Pérez, P. How Different Are Nitrile Oxides from Nitrones in zw-type [3+2] Cycloaddition Reactions? A Molecular Electron Density Theory Study. *J. Org. Chem.*, **2025**, *90*, 3936−3950.

[23] Domingo, L. R.; Pérez, P. Unveiling the Role of the Lewis Acids in the Acceleration of Alder–Ene Reactions: A Molecular Electron Density Theory Study. *Molecules*, **2025**, *30*, 4289.

[24] Domingo, L. R.; Pérez, P., Ríos-Gutiérrez, M.; José Aurell, M. Advanced Molecular Electron Density Theory Study of the Substituent Effects in Nucleophilic Substitution Reactions. *ACS Omega*, **2025**, *10*, 30194−30206.

[25] Domingo, L. R.; Aurell, M. J.; Pérez, P. Unveiling the Electronic Effects of the Lewis Acids in Nucleophilic Substitution Reactions: A Molecular Electron Density Theory Study. *J. Org. Chem.* (**2025**) *submitted*.

[26] Rowley, D.; Steiner, H. Kinetics of diene reactions at high temperatures. *Discuss Faraday Soc.*, **1951**, *10*, 198–213.

[27] Woodward, R. B.; Hoffmann, R. The Conservation of Orbital Symmetry. *Angew. Chem. Int. Ed. Engl.*, **1969**, *8*, 781–853.

[28] Houk, K. N.; Gonzalez, J.; Li, Y. Pericyclic Reaction Transition States: Passions and Punctilios, 1935-1995*. Acc. Chem. Res.*, **1995**, *28*, 81-90.

[29] Carey, F.A.; Sundberg, R. J. in *Advanced Organic Chemistry. Part A: Strucutre and Mechanisms*; fifth Edition ed.; Springer: New York, 2007.

[30] Martín Pendás, A.; Blanco, M.A.; Francisco, E. Chemical Fragments in Realpace: Definitions, Properties and Energetic Decompositions. *J. Comput.Chem.*, **2007**, *28*, 161–184.

[31] Triestram, L.; Falcioni, F.; Popelier P.L.A., Interacting Quantum Atoms and Multipolar Electrostatic Study of XH···π Interactions. *ACS Omega*, **2023**, *8,* 34844–34851.

[32] Berski, S.; Andrés, J.; Silvi, B.; Domingo, L.R. The joint use of catastrophe theory and electron localization function to characterize molecular mechanisms. A density functional study of the Diels-Alder reaction between ethylene and 1,3-butadiene. *J. Phys. Chem. A*, **2003**, *107*, 6014-6024.

[33] Domingo, L.R. A new C–C bond formation model based on the quantum chemical topology of electron density. *RSC Adv.*, **2014**, *4*, 32415–32428.

[34] Domingo, L.R.; Ríos-Gutiérrez, M. A Useful Classification of Organic Reactions Bases on the Flux of the Electron Density. *Sci. Rad.*, **2023**, *2*, 1.

[35] Domingo, L.R.; Sáez, J.A. Understanding the Mechanism of the Polar Diels-Alder Reaction. *Org. Biomol. Chem.*, **2009**, *7*, 3576-3583.

[36] *AIMAll* (Version 19.10.12), Keith, T. A. TK Gristmill Software, Overland Park KS, USA, 2019 (aim.tkgristmill.com).

[37] Hamlin, T.A.; Bickelhaupt, F.M.; Fernández, I. The Pauli Repulsion-Lowering Concept in Catalysis. *Acc. Chem. Res.*, **2021**, *54*, 1972−1981.

[38] Becke, A.D. Density-functional thermochemistry. III. The role of exact exchange. *J. Chem. Phys.*, **1993**, *98*, 5648–5652.

[39] Lee, C.; Yang, W.; Parr, R.G. Development of the Colle-Salvetti correlation-energy formula into a functional of the electron density. *Phys. Rev. B*, **1988**, *37*, 785–789.

[40] Hehre, M. J.; Radom, L.; Schleyer, P.v.R.; Pople, J. in *Ab initio Molecular Orbital Theory*. Wiley, New York, 1986.

[41] Reed, A.E.; Weinstock, R. B.; Weinhold, F. Natural population analysis. *J. Chem. Phys.*, **1985**, *83*, 735–746.

[42] Reed, A. E.; Curtiss, L.A.; Weinhold, F. Intermolecular interactions from a natural bond orbital, donor-acceptor viewpoint. *Chem. Rev.*, **1988**, *88*, 899–926.

[43] Frisch, M. J.; Trucks, G. W.; Schlegel, H. B.; Scuseria, G. E.; Robb, M. A.; Cheeseman, J. R.; Scalmani, G.; Barone, V.; Mennucci, B.; Petersson, G. A.; Nakatsuji, H.; Li, X.; Caricato, M.; Marenich, A. V.; Bloino, J.; Janesko, B. G.; Gomperts, R.; Mennucci, B.; Hratchian, H. P.; Ortiz, J. V.; Izmaylov, A. F.; Sonnenberg, J. L.; Williams-Young, D.;

Ding, F.; Lipparini, F.; Egidi, F.; Goings, J.; Peng, B.; Petrone, A.; Henderson, T.; Ranasinhe, D.; Zakrzewski, V. G.; Gao, J.; Rega, N.; Zheng, G.; Liang, W.; Hada, M.; Ehara, M.; Toyota, K.; Fukuda, R.; Hasegawa, J.; Ishida, M.; Nakajima, T.; Honda, Y.; Kitao, O.; Nakai, H.; Vreven, T.; Throssell, K.; Montgomery, J. A., Jr.; Peralta, J. E.; Ogliaro, F.; Bearpark, M.; Heyd, J. J.; Brothers, E. N.; Kudin, K. N.; Staroverov, V. N.; Keith, T. A.; Kobayashi, R.; Normand, J.; Raghavachari, K.; Rendell, A.; Burant, J. C.; Iyengar, S. S.; Tomasi, J.; Cossi, M.; Millam, J.M.; Klene, M.; Adamo, C.; Cammi, R.; Ochterski, J. W.; Martin, R. L.; Morokuma, K.; Farkas, Ö .; Foresman, J. B.; Fox, D. J.; Gaussian 16, Revision A.03; Gaussian, Inc.; Wallingford CT, 2017.

[44] *GaussView*, Version 6.0, R. Dennington, Keith, T. A.; Millam, J. M. Semichem Inc., Shawnee Mission, KS, 2016.

[45] Noury, S.; Krokidis, X.; Fuster, F.; Silvi, B. Computational tools for the electron localization function topological analysis. *Comput. Chem.*, **1999**, *23*, 597–604.

[46] Zhao, Y.; Truhlar, D. G. The M06 suite of density functionals for main group thermochemistry, thermochemical kinetics, noncovalent interactions, excited states, and transition elements: two new functionals and systematic testing of four M06-class functionals and 12 others functional. *Theor. Chem. Acc.*, **2008**. *120*, 215–241.